ASTRONOMY

Discovery of diffuse optical emission lines from the inner Galaxy: Evidence for LI(N)ER-like gas

D. Krishnarao[1]*, R. A. Benjamin[2], L. M. Haffner[3,4,1]

Optical emission lines are used to categorize galaxies into three groups according to their dominant central radiation source: active galactic nuclei, star formation, or low-ionization (nuclear) emission regions [LI(N)ERs] that may trace ionizing radiation from older stellar populations. Using the Wisconsin H-Alpha Mapper, we detect optical line emission in low-extinction windows within eight degrees of Galactic Center. The emission is associated with the 1.5-kiloparsec-radius "Tilted Disk" of neutral gas. We modify a model of this disk and find that the hydrogen gas observed is at least 48% ionized. The ratio [NII] λ6584 angstroms/Hα λ6563 angstroms increases from 0.3 to 2.5 with Galactocentric radius; [OIII] λ5007 angstroms and Hβ λ4861 angstroms are also sometimes detected. The line ratios for most Tilted Disk sightlines are characteristic of LI(N)ER galaxies.

INTRODUCTION

Evidence for ionized gas in galaxies has existed since 1909 when optical emission lines were first detected in the spectra of a "spiral nebula" (*1*). Motivated by the discovery that the redshift of spectral lines of galaxies correlated with their distance (*2*), teams at Mt. Wilson Observatory and Lick Observatory began programs to obtain spectra for a large sample of these galaxies. Early on, both groups detected [OII] λ3727-Å emission from diffuse ionized gas in the inner regions ($R < 2$ kpc) of several galaxies (*3*, *4*). Subsequent observations showed that this gas was characterized by a [NII] λ6584 Å/Hα λ6563 Å line ratio greater than unity, as opposed to the value of 0.3 seen in ionized gas surrounding HII regions in galaxy disks (*5*).

Emission line studies of ionized gas in subsequent decades focused on the nuclear regions ($R < 0.5$ kpc) of galaxies, leading to the classification of galaxies according to their emission line ratios. The line ratios [NII] λ6584 Å/Hα λ6563 Å and [OIII] λ5007 Å/Hβ λ4861 Å were found to be particularly useful in classifying galaxies according to the principal source of ionization (*6*). When combined with models of the radiation field, these line ratios allowed galaxies to be classified into one of three categories according to the dominant source of radiation: star formation, active galactic nuclei, or low-ionization (nuclear) emission line regions [LI(N)ERs] (*7*–*9*). This third category was introduced by Heckman (*10*); possible sources of ionization included shocks, cooling flows, and photoionization by evolved stellar populations (*11*).

Modern investigations of LI(N)ER emission (*12*–*14*) have resurrected interest in the radial extent of this gas, leading to the suggestion that the "nuclear" designation be dropped. Supporting this view, similar emission line ratios are found in the extended regions of elliptical and early-type galaxies, which also show evidence for an ultraviolet (UV) upturn. This UV upturn was first detected in the inner regions of M31 by Code (*15*), who speculated that it could be responsible for the previously observed diffuse ionized gas (*16*, *17*). Stellar evolution and photoionization modeling of evolved stellar populations show that both the UV upturn and the optical emission line ratios may be explained by a population of hot old low-mass evolved stars [e.g., (*18*) and references therein]. There are several classes of potential ionizing sources, e.g., post–asymptotic giant branch (AGB) stars, AGB manqué stars, hot white dwarfs, pre-planetary nebula stars, and extreme horizontal branch/subdwarf OB stars, but the relative contributions of these sources to the total ionizing flux have not been definitively established. Since many of these sources are faint, it is not possible to resolve them in extragalactic systems. Even in M31—up until now, the nearest LI(N)ER—it is extremely challenging to detect individual sources and establish their contribution to the hydrogen-ionizing flux.

Here, we report the first detection of optical emission LI(N)ER-type gas in the inner part of the Milky Way Galaxy using the Wisconsin H-Alpha Mapper (WHAM) (*19*, *20*). Our measurement of these optical emission lines in the inner Galaxy is possible due to two fortuitous circumstances. First, the neutral gas layer between Galactocentric radii of 0.5 kpc < R_G < 1.5 kpc is tilted (*21*), extending more than 5° below the Galactic plane in Galactic longitudes $l = +10°$ to 0°. Second, this structure aligns with several low-extinction directions toward Galactic Center around $(l,b) = (1° \text{ to } 5°, -3° \text{ to } -6°)$, including Baade's Window. This tilted gas structure is distinct from the "Central Molecular Zone" (CMZ) interior to $R_G \sim 0.5$ kpc, which is also tilted, but with a different rotational axis.

We find three principal results. First, the optical line ratios for this gas are unlike anywhere else in the Milky Way Galaxy but typical of emission from LI(N)ER systems. Second, the inferred mass of ionized gas is much higher than predicted by current hydrodynamical models of gas flowing in a Milky Way–barred potential. A tilted geometrical model of the neutral gas modified to include an ionized component suggests that the atomic (nonmolecular) gas in the inner Galaxy is more than 50% ionized. And third, the [NII] λ6584 Å/Hα λ6563 Å ratio increases with Galactocentric radius, suggesting a radiation field that changes with position in the inner Galaxy. In the future, these observations may be compared with spatially resolved observations of UV-emitting stellar populations to assess the source of ionization for LI(N)ER-type gas.

RESULTS

Using the WHAM (*19*, *20*), we obtained high sensitivity ($I_{H\alpha} \sim 0.1$ *R*), velocity-resolved ($R \sim 25{,}000$; $\Delta v \sim 12$ km s^{-1}) observations of several

[1]Department of Astronomy, University of Wisconsin-Madison, 475 N Charter St., Madison, WI 53706, USA. [2]Department of Physics, University of Wisconsin-Whitewater, 800 West Main Street, Whitewater, WI 53190, USA. [3]Department of Physical Sciences, Embry Riddle Aeronautical University, 1 Aerospace Blvd., Daytona Beach, FL 32114, USA. [4]Space Science Institute, 4750 Walnut St., Suite 205, Boulder, CO 80301, USA.
*Corresponding author. Email: krishnarao@astro.wisc.edu

optical emission lines, e.g., Hα λ6563 Å, Hβ λ4861 Å, [NII] λ6584 Å, and [OIII] λ5007 Å, in the vicinity of Galactic Center. This dual-etalon Fabry-Perot spectrometer samples the region using a 1° diameter beam. These data are supplemented with HI 21-cm observations from the HI4PI survey (*22*), with a sensitivity of 43 mK and an angular resolution of 16.2 arcmin.

In the low-extinction region around $(l,b) = (1° \text{ to } 5°, -3° \text{ to } -6°)$, we detect Hα emission in the velocity range of $-110 \text{ km s}^{-1} \leq v_{\text{LSR}} \leq -50 \text{ km s}^{-1}$, the same velocity range in which 21-cm emission is seen. Figure 1 shows a map of HI 21-cm emission near Galactic Center for longitude $l > 0°$, with $-110 \text{ km s}^{-1} \leq v_{\text{LSR}} \leq -50 \text{ km s}^{-1}$ in blue and $l < 0°$ with $+50 \text{ km s}^{-1} \leq v_{\text{LSR}} \leq +110 \text{ km s}^{-1}$ in red. These "forbidden" velocities cannot arise from circular rotation in the inner Galaxy and have been interpreted as the expansion of a tilted circular annulus (*21*) or tilted elliptical trajectories of gas, possibly aligned with the bar (*23*). The contours on the HI 21-cm map show our detection of Hα emission in the same velocity windows. Two example spectra show kinematically distinct optical emission lines in the same velocity range as the neutral gas of the Tilted Disk. There is also Hα emission above the midplane of the Tilted Disk that we refer to as the "Upper Feature." Unlike the Tilted Disk emission, this emission is not kinematically distinct and is found in broad wings of local Hα emission. In some directions, we observe HI 21-cm emission at the same negative velocities as the Upper Feature, but this emission will not be considered further.

Figure 1 also shows that the [NII]/Hα emission line ratio associated with the Tilted Disk is substantially higher than the local emission traced by gas near $v_{\text{LSR}} = 0 \text{ km s}^{-1}$. Our multiwavelength WHAM observations of [NII], [OIII], Hα, and Hβ allow for the inner regions of the Milky Way to be compared with other galaxies using the diagnostic Baldwin-Phillips-Terlevich (BPT) diagram (*6*). Figure 2 shows two optical line ratios in a diagram comparing Sloan Digital

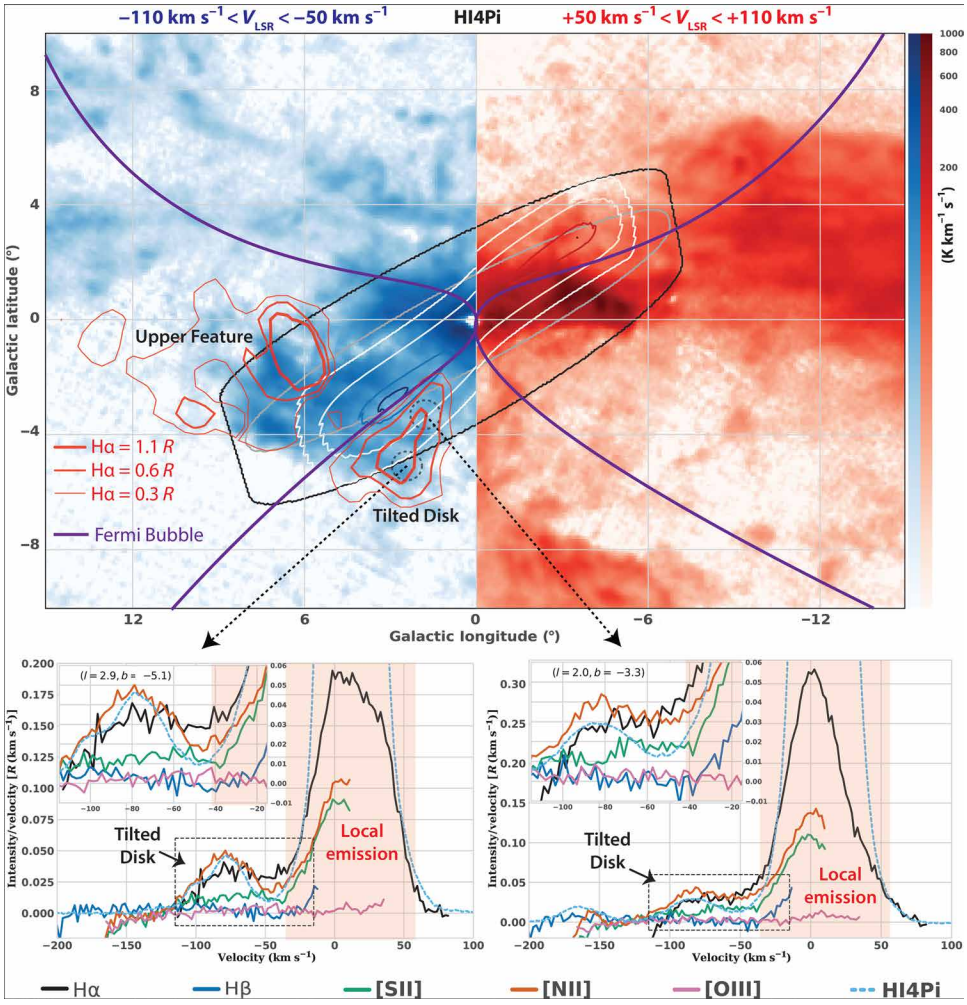

Fig. 1. Observations of the Tilted Disk. Integrated velocity channel map of HI 21-cm emission over inner Galaxy forbidden velocities for positive longitudes ($-110 \text{ km s}^{-1} \leq v_{\text{LSR}} \leq -50 \text{ km s}^{-1}$; bluescale) and negative longitudes ($+50 \text{ km s}^{-1} \leq v_{\text{LSR}} \leq +110 \text{ km s}^{-1}$; redscale), showing the tilted distribution of this gas. Hα contours integrated over the same velocity range show evidence for an ionized counterpart to the neutral gas. A projection of a tilted elliptical HI disk model (*23*) integrated over all velocities is shown with black and gray contours, while the blue-to-white and red-to-white contours show the emission predicted by the model in the same velocity range as the data with contour values of 0.1, 10, 75, and 100 K km^{-1} s^{-1}. The purple line shows the projected outline of the Fermi Bubble (*38*) extrapolated into Galactic Center. The dotted circles and arrows show the location of two 1° WHAM beams and their corresponding optical emission line spectra for Hα, Hβ, [NII], [SII], and [OIII]. A rescaled (1/20) HI spectrum averaged over the WHAM beam is also shown to demonstrate the kinematic agreement between the neutral and ionized gas observations. The bright emission around $v_{\text{LSR}} = 0 \text{ km s}^{-1}$ is from local emission in the solar neighborhood.

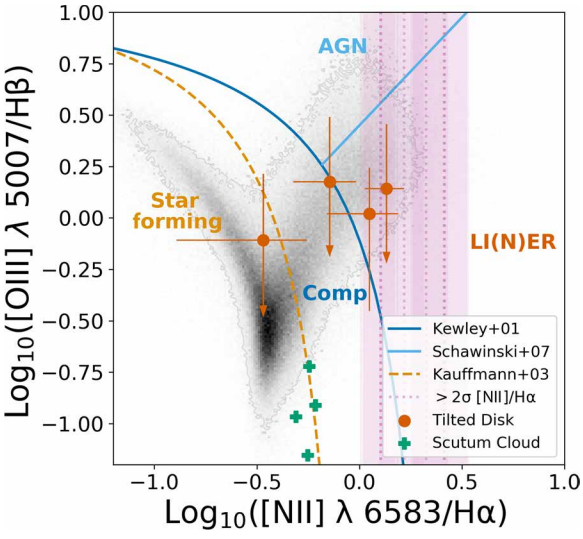

Fig. 2. BPT diagram with the Milky Way. BPT diagram of the [OIII]/Hβ versus [NII]/Hα line ratios for SDSS DR7 galaxies (grayscale) and the Milky Way (colored data), as observed with WHAM. Classification lines in blue, cyan, and orange separate regions by their modeled primary excitation mechanism (*7*–*9*). Orange-shaded filled circles are WHAM observations of the Tilted Disk structure we have modeled. Green plus symbols are extinction-corrected WHAM observations of the Scutum direction (*24*) and cover a range of 4 kpc < R_G < 7 kpc. Pink lines and shaded regions show additional observations of [NII]/Hα of the Tilted Disk where either [OIII] or Hβ are not detected. Error bars are either 1σ errors or upper limits (arrows).

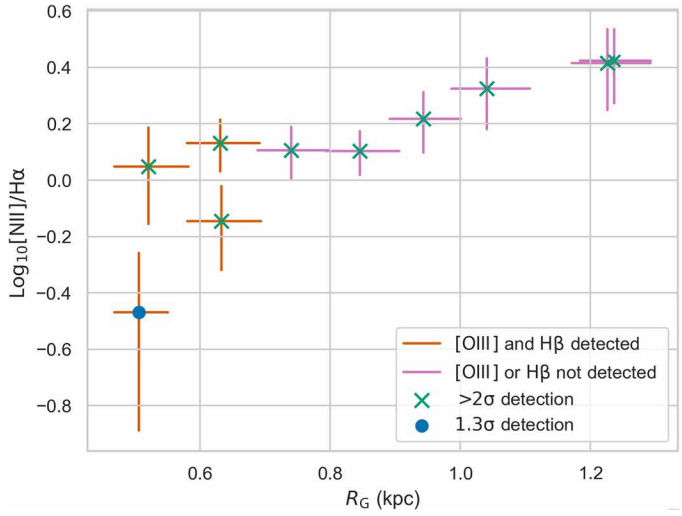

Fig. 3. [NII]/Hα versus Galactocentric radius. [NII]/Hα line ratio toward the Tilted Disk as a function of Galactocentric radius (R_G). Points with orange error bars correspond to the orange points in the BPT diagram of Fig. 2, while points with pink error bars correspond to the pink vertical bars in the BPT diagram. An additional offset along both axes of 0.01 is added to the point with the largest values on both axes to differentiate the two points with very similar values.

Sky Survey (SDSS) galaxies, WHAM observations of the Tilted Disk, and WHAM observations in the direction of the "Scutum Star Cloud", an extinction window at $l \sim 30°$, which traces gas in the Scutum spiral arm at $R_G = 4$ to 6 kpc (*24*). Of the 10 Tilted Disk pointings shown on this plot (orange points and pink bars), 6 have only [NII]/Hα ratio measurements, 3 have upper limits for [OIII]/Hβ, and 1 pointing has both lines of the [OIII]/Hβ ratio detected at greater than 2σ significance. All but one of these pointings would be classified as composite or LI(N)ER emission. Moreover, the [NII]/Hα ratio is distinctly different from what is seen in HII regions, Galactic diffuse ionized gas in the disk, and the Scutum spiral arm but is similar to ratios seen in LI(N)ERs. Last, the face-on Hα surface brightness predicted by a geometric model of the ionized Tilted Disk (described in the next section) is ~5×10^{-17} ergs s^{-1} cm^{-2} $arcsec^{-2}$, comparable to the average surface brightness observed in M31 (*25*).

Using the same geometrical model to convert observed velocity to Galactocentric radius, Fig. 3 also shows evidence for a trend of increasing [NII]/Hα ratio with Galactocentric radius in the inner Galaxy. We also find that the spectra in the direction closest to Galactic Center are consistent with star formation–dominated spectra.

Interpreting these emission spectra further requires a three-dimensional (3D) kinematic model of gas to convert the observed gas velocity to the gas location within the Galaxy and to estimate the total ionized gas mass. We consider two different models: (i) a geometrical model of a tilted elliptical disk (*23*), modified to include an ionized gas component, and (ii) a hydrodynamical model of gas flow in the barred potential of the Milky Way (*26*) that includes heating, cooling, and a chemical network to track the ionization state and composition of the gas. Details for both models are given in the Supplementary Materials and are summarized here.

We first consider a previously constructed model of the neutral Tilted Disk by Liszt and Burton (*23*) and modify it to include an ionized gas component. Before the development of this model, anomalous velocity features were modeled as arising in explosive events at Galactic Center (*27*). The original Tilted Disk model (*21*) explained many of these observations as resulting from a tilted disk with radial expansion. Subsequent refinements of the model explained the anomalous velocity gas as elliptical motion requiring no expansion (*23*).

The neutral gas model has elliptical streamlines of gas, with a semimajor axis of $a_d' = 1.51$ kpc and a semiminor axis of $b_d' = 0.49$ kpc. The gas density varies only as a function of height; angular momentum is conserved along the elliptical orbits. The disk is tilted 13.5° out of the plane, 20° toward us, and has its major axis at an angle of 48.5° with respect to the Sun–Galactic Center direction (*23*). Our best-fitting ionized gas density model uses the same orientation and velocity field as the neutral gas and is characterized by a central midplane density $n_{e,0} = 0.39$ (+0.06/−0.05) cm^{-3} and central Gaussian scaleheight, $H_{z,0} = 0.26 \pm 0.04$ kpc. We also introduce a flaring factor, $F_z = 2.05$ (+0.42/−0.31), such that the scaleheight increases linearly with radius as $H_z(r) = H_{z,0}[(1 - x) + F_z\, x]$ where $x = r/(a_d')$. Similar to the neutral gas model, we assume that surface density is independent of radius, so $n_e(r) = n_{e,0}\, H_{z,0}/H_z(r)$. As in previous work (*28*), we remove an inner ellipse with a semimajor/minor axes of $a_d'/2$ and $b_d'/2$, half the outer value.

This model predicts the observational trends of Hα seen with WHAM and confirms that directions where we do not detect emission are inaccessible due to extinction. The previous neutral gas model and our new ionized gas model allow us to compare the mass of these two components. We find a total neutral gas mass of $M_{H0} = (3.1 \pm 0.3) \times 10^6$ solar masses, which agrees with previous estimates (*28*). The total ionized gas mass from our model is $M_{H+} = 12$ (+4/−3) × 10^6 solar masses. Since these values come from extrapolating our ionized gas model beyond the observational window where Hα is

detected, we also compare the total mass of neutral and ionized gas in our observing window. Over the region, $l = 0°$ to $6°$, $b = -7°$ to $-2°$ in the velocity interval, $v_{LSR} = -120$ to -40 km s^{-1}, HI 21-cm observations combined with our geometric models yield a neutral and ionized gas mass of $(0.30 \pm 0.01) \times 10^6$ and $0.37\ (+0.12/-0.09) \times 10^6$ solar masses, respectively, and an ionization fraction of 55% (±7%). Despite the uncertainties of how to extrapolate our results in the extinction window to the full structure, it is clear that a substantial fraction of the gas we observe is ionized. Details on the mass estimates and uncertainties shown here are available in the Supplementary Materials.

Although the geometric model has the advantage of simplicity, it does not capture the full complexity of the gas distribution expected in a barred galaxy like the Milky Way. In particular, hydrodynamical models show notable variations in density with both azimuth and radius interior to the bar radius [e.g., (*26*) and references therein]. From our vantage point at the Sun, looking in the direction of positive Galactic longitudes ($l > 0°$), these models predict that the leading—high positive v_{LSR}—side of the bar is characterized by dense gas and dust, while the trailing side of the bar—high negative v_{LSR}—would have much lower gas density. To examine the effects of this density asymmetry on our interpretation, the Supplementary Materials contains a comparison of our geometric model to a hydrodynamical simulation (*26*). Since this particular simulation also tracks the chemical state of the gas, it makes specific predictions for the density structure of ionized gas.

We find that this model fails to adequately account for the Hα emission we see in three principal ways. First, it fails to predict the observed tilted distribution of gas, a shortcoming discussed in (*26*). Since the model gas layer lies in the plane, it lies behind large amounts of extinction, and we would expect to detect no Hα. Second, although the vertical thickness of the gas depends on position and is not easily characterizable with a single scaleheight, we find that at all positions, the model produces a gas layer much thinner than what is inferred from both the Hα and HI observations. This issue was also noted by (*26*) with regard to the molecular and neutral atomic gas but is even more discrepant for the ionized gas component. Last, even when we introduced an arbitrary tilt in the gas distribution, we found that the gas on the trailing side of the bar, traced by negative-velocity gas, had a much lower density of ionized gas than needed to explain the observed Hα emission. This last discrepancy is almost certainly due to the radiation field used in this simulation, which did not include hydrogen-ionizing photons. All of the hydrogen ionization in this model comes from cosmic rays or collisional ionization.

The discrepancies we identify are likely to be present in any of the currently available models of gas flow in a barred potential. To our knowledge, no model has successfully resulted in a tilted distribution. Moreover, in all models, the higher gravitational potential of the inner Galaxy can be expected to result in a thin gas layer in the absence of other sources of vertical support. While many models seem to produce a high positive-velocity dense gas structure on the leading side of the bar, analogous to the observed "Connecting Arm" seen in CO observations, there has been much less attention paid to matching the column densities of gas in the negative-velocity trailing side of the bar. Regardless, both our geometrical model and the hydrodynamical models agree on the general location within the Galaxy where the kinematic signatures we observe must originate—the trailing side of the bar.

DISCUSSION

Given that the presence of LI(N)ER-type gas has been shown to be well-correlated with the occurrence of Galactic bars (*29*), one might have reasonably suspected the ionized gas in the inner Milky Way to have LI(N)ER-like line ratios. Our observations not only confirm this expectation but allow for new constraints on the nature of the ionization mechanism and the power requirements. Particularly intriguing is our finding that the [NII]/Hα ratio drops as the Galactocentric radius decreases, with our innermost observations consistent with a star formation–dominated ionizing radiation field. Analysis of far-infrared line ratios in the CMZ, which are not accessible optically, has been interpreted as a star formation–dominated radiation field (*30*), although the situation is not entirely clear (*31*).

With the caveat that the true density structure of ionized gas is likely to be more complicated than assumed in our geometric model, we can use our Hα observations to infer the level of ionizing flux in the inner Galaxy. If one assumes that the disk is ionized from outside, then a balance between the number of ionizations and recombinations in our model exponential ionized disk implies a (plane-parallel) hydrogen-ionizing flux of $\phi = (2.7 \times 10^7$ photons s^{-1} cm^{-2}) $(1 - 0.5\times)$ to each side of the disk, where $x = r/a_d'$. This is 10 times the flux needed to maintain the warm ionized layer in the vicinity of the Sun (*32*). The corresponding luminosity of hydrogen-ionizing photons is $Q(H^0) = 6.3 \times 10^{50}$ photons s^{-1}. This can be compared to the number of Lyman continuum photons coming from star formation in the CMZ, which is $Q_{CMZ} = 1.2$ to 3.5×10^{52} photons s^{-1}, assuming a CMZ star formation rate of 0.05 to 0.15 solar mass year^{-1} (*33*, *34*) and that a star formation rate of 1 solar mass year^{-1} produces 2.4×10^{53} photons s^{-1} (*35*).

Although it would only take approximately 5 to 10% of these ionizing photons to maintain the ionization in the Tilted Disk, models of radiative transfer will be needed to establish whether this radiation source alone would suffice to explain the changing level of ionization seen. Evolved stellar populations, e.g., subdwarf OB stars, have been posited as a source of ionization in LI(N)ER systems; the contribution of these sources could be observationally constrained in the Galaxy. A Galactic bulge concentration of these stars would occur at magnitude $m_V \sim 19$ for a subdwarf OB absolute magnitude of $M_V = 4.6$ (*36*). Since the Galactic bulge is vertically thicker than much of the extinction in the inner Galaxy, such a population could be detected.

Absorption line studies will also be valuable for studying the thermal pressure, ionization, metallicity, and dust depletion in the neutral and ionized components of this LI(N)ER-like gas. One such study toward the distant B1 Ib-II star LS 4825 ($l = 1.67°$ and $b = -6.63°$) shows absorption at the same velocity as the Tilted Disk. Analysis of this component yields a solar abundance of sulfur, ~1-dex depletion of iron and aluminum, a thermal pressure three times higher than in the solar neighborhood, and evidence for more highly ionized gas traced by C IV and Si IV, indicating a possible interface with hotter gas (*37*).

Last, hot gas associated with a large-scale nuclear outflow indicated by the Fermi Bubbles may provide another source of ionizing radiation (*38*). In Fig. 1, we show how the estimated boundary of the Fermi Bubble—as seen in gamma-ray and x-ray emission—compares to the structure of the Tilted Disk. If hot gas is intermixed with the Tilted Disk structure, then our gas mass estimates based on Hα emission will be lower limits (*39*) to the total amount of ionized gas in the inner Galaxy. Our observations show that the nearest

LI(N)ER-like gas to us in the universe is now the inner Milky Way and no longer the inner parts of M31. This opens new avenues to better constrain the nature and ionization sources of this elusive class of gas with an unprecedented level of detail across all wavelengths.

MATERIALS AND METHODS

All data used in this work can be accessed publicly. The WHAM Sky Survey has a public release of Hα observations available online at http://www.astro.wisc.edu/wham-site/. The HI4PI observations of 21-cm neutral hydrogen (*22*) and the 3D dust models (*40*) used in this work are also available publicly. The Tilted Disk geometric model can be computed using the open-source Python package, modspectra (https://github.com/Deech08/modspectra). Multi-wavelength WHAM observations have not been publicly released, but those specific to this work can be accessed at the following GitHub repository, which also includes Python notebooks to replicate plots shown in this work (https://github.com/Deech08/mw_bpt).

Statistical analysis

For each WHAM pointing, the Hα emission intensity and line profiles are calculated for our model assuming Case B recombination and using maps of the 3D dust distribution to apply extinction corrections (*40*). A Bayesian Markov Chain Monte Carlo approach is used to optimize the model in comparison with WHAM observations of Hα in the extinction windows shown in Fig. 1. Our model predicts the observational trends of Hα seen with WHAM and confirms that directions where we do not detect emission are inaccessible due to extinction. Full details on this procedure are available in the Supplementary Materials.

SUPPLEMENTARY MATERIALS

Supplementary material for this article is available at http://advances.sciencemag.org/cgi/content/full/6/27/eaay9711/DC1

REFERENCES AND NOTES

1. E. A. Fath, The spectra of some spiral nebulae and globular star clusters. *Publ. Astron. Soc. Pac.* **21**, 138–143 (1909).
2. E. Hubble, A relation between distance and radial velocity among extra-galactic nebulae. *Proc. Natl. Acad. Sci. U.S.A.* **15**, 168–173 (1929).
3. M. L. Humason, The apparent radial velocities of 100 extra-galactic nebulae. *Astrophys. J.* **83**, 10 (1936).
4. N. U. Mayall, A low-dispersion UV glass spectrograph for the crossley reflector. *Publ. Astron. Soc. Pac.* **48**, 14 (1936).
5. E. M. Burbidge, G. R. Burbidge, Ionized gas in spiral and irregular galaxies. *Astrophys. J.* **135**, 694 (1962).
6. J. A. Baldwin, M. M. Phillips, R. Terlevich, Classification parameters for the emission-line spectra of extragalactic objects. *Publ. Astron. Soc. Pac.* **93**, 5 (1981).
7. L. J. Kewley, M. A. Dopita, R. S. Sutherland, C. A. Heisler, J. Trevena, Theoretical modeling of starburst galaxies. *Astrophys. J.* **556**, 121 (2001).
8. G. Kauffmann, T. M. Heckman, C. Tremonti, J. Brinchmann, S. Charlot, S. D. M. White, S. E. Ridgway, J. Brinkmann, M. Fukugita, P. B. Hall, Ž. Ivezić, G. T. Richards, D. P. Schneider, The host galaxies of active galactic nuclei. *Mon. Not. R. Astron. Soc.* **346**, 1055–1077 (2003).
9. K. Schawinski, D. Thomas, M. Sarzi, C. Maraston, S. Kaviraj, S.-J. Joo, S. K. Yi, J. Silk, Observational evidence for AGN feedback in early-type galaxies. *Mon. Not. R. Astron. Soc.* **382**, 1415–1431 (2007).
10. T. M. Heckman, An optical and radio survey of the nuclei of bright galaxies. Activity in normal galactic nuclei. *Astron. Astrophys.* **87**, 152–164 (1980).
11. A. V. Filippenko, Physics of liners in view of recent observations. *Astron. Soc. Pac. Conf.* **103**, 17 (1996).
12. R. G. Sharp, J. Bland-Hawthorn, Three-dimensional integral field observations of 10 galactic winds. I. extended phase (gsim10 Myr) of mass/energy injection before the wind blows. *Astrophys. J.* **711**, 818–852 (2010).
13. F. Annibali, A. Bressan, R. Rampazzo, W. W. Zellinger, O. Vega, P. Panuzzo, Nearby early-type galaxies with ionized gas. IV. Origin and powering mechanism of the ionized gas. *Astron. Astrophys.* **519**, 31 (2010).
14. F. Belfiore, R. Maiolino, C. Maraston, E. Emsellem, M. A. Bershady, K. L. Masters, R. Yan, D. Bizyaev, M. Boquien, J. R. Brownstein, K. Bundy, N. Drory, T. M. Heckman, D. R. Law, A. Roman-Lopes, K. Pan, L. Stanghellini, D. Thomas, A.-M. Weijmans, K. B. Westfall, SDSS IV MaNGA–Spatially resolved diagnostic diagrams: A proof that many galaxies are LIERs. *Mon. Not. R. Astron. Soc.* **461**, 3111 (2016).
15. A. D. Code, Photoelectric photometry from a space vehicle. *Publ. Astron. Soc. Pac.* **81**, 475 (1969).
16. H. W. Babcock, The rotation of the Andromeda Nebula. *Lick Observatory Bull.* **498**, 41–51 (1939).
17. G. Munch, Motions of the gas near the nucleus of M31. *Astrophys. J.* **65**, 55 (1960).
18. N. Byler, J. J. Dalcanton, C. Conroy, B. D. Johnson, J. Choi, A. Dotter, P. Rosenfield, Self-consistent predictions for LIER-like emission lines from post-AGB stars. *Astron. J.* **158**, 2 (2019).
19. L. M. Haffner, R. J. Reynolds, S. L. Tufte, G. J. Madsen, K. P. Jaehnig, J. W. Percival, The Wisconsin Hα Mapper Northern Sky Survey. *Astrophys. J. Suppl. S.* **149**, 405–422 (2003).
20. L. M. Haffner, R. J. Reynolds, G. J. Madsen, A. S. Hill, K. A. Barger, K. P. Jaehnig, E. J. Mierkiewicz, J. W. Percival, N. Chopra, Early results from the Wisconsin H-Alpha Mapper Southern Sky Survey, in *Proceedings of the Dynamic Interstellar Medium: A Celebration of the Canadian Galactic Plane Survey* (Astronomical Society of the Pacific, 2010), 388 p.
21. W. B. Burton, H. S. Liszt, The gas distribution in the central region of the Galaxy. I - Atomic hydrogen. *Astrophys. J.* **225**, 815–842 (1978).
22. HI4PI Collaboration, N. B. Bekhti, L. Flöer, R. Keller, J. Kerp, D. Lenz, B. Winkel, J. Bailin, M. R. Calabretta, L. Dedes, H. A. Ford, B. K. Gibson, U. Haud, S. Janowiecki, P. M. W. Kalberla, F. J. Lockman, N. M. McClure-Griffiths, T. Murphy, H. Nakanishi, D. J. Pisano, L. Staveley-Smith, HI4PI: A full-sky H I survey based on EBHIS and GASS. *Astron. Astrophys.* **594**, 15 (2016).
23. H. S. Liszt, W. B. Burton, The gas distribution in the central region of the Galaxy. III - A barlike model of the inner-Galaxy gas based on improved H I data. *Astrophys. J.* **236**, 779–797 (1980).
24. G. J. Madsen, R. J. Reynolds, An investigation of diffuse interstellar gas toward a large, low-extinction window into the inner Galaxy. *Astrophys. J.* **630**, 925–944 (2005).
25. V. C. Rubin, W. Kent Ford Jr., Radial velocities and line strengths of emission lines across the nuclear disk of M31. *Astrophys. J.* **170**, 25 (1971).
26. M. C. Sormani, R. G. Treß, M. Ridley, S. C. O. Glover, R. S. Klessen, J. Binney, J. Magorrian, R. Smith, A theoretical explanation for the Central Molecular Zone asymmetry. *Mon. Not. R. Astron. Soc.* **475**, 2383–2402 (2018).
27. J. H. Oort, The galactic center. *Annu. Rev. Astron. Astrophys.* **15**, 295–362 (1977).
28. K. Ferrière, W. Gillard, P. Jean, Spatial distribution of interstellar gas in the innermost 3 kpc of our galaxy. *Astron. Astrophys.* **467**, 611–627 (2007).
29. P. A. James, S. M. Percival, Discovery of kpc-scale line emission in barred galaxies, not linked to AGN or star formation. *Mon. Not. R. Astron. Soc.* **450**, 3503–3513 (2015).
30. D. An, S. V. Ramírez, K. Sellgren, The Galactic Center: Not an active galactic nucleus. *Astrophys. J. Suppl.* **206**, 20 (2013).
31. J. P. Simpson, Spitzer infrared spectrograph observations of the Galactic Center: Quantifying the extreme ultraviolet/soft x-ray fluxes. *Astrophys. J.* **857**, 59 (2018).
32. R. J. Reynolds, The power requirement of the free electron layer in the Galactic disk. *Astrophys. J. Lett.* **349**, L17 (1990).
33. R. M. Crocker, Non-thermal insights on mass and energy flows through the Galactic Centre and into the *Fermi* bubbles. *Mon. Not. R. Astron. Soc.* **423**, 3512–3539 (2012).
34. S. N. Longmore, J. Bally, L. Testi, C. R. Purcell, A. J. Walsh, E. Bressert, M. Pestalozzi, S. Molinari, J. Ott, L. Cortese, C. Battersby, N. Murray, E. Lee, J. M. D. Kruijssen, E. Schisano, D. Elia, Variations in the Galactic star formation rate and density thresholds for star formation. *Mon. Not. R. Astron. Soc.* **429**, 987–1000 (2013).
35. J. Bland-Hawthorn, P. R. Maloney, R. S. Sutherland, G. J. Madsen, Fossil imprint of a powerful flare at the Galactic Center along the Magellanic stream. *Astrophys. J.* **778**, 58 (2013).
36. S. Geier, R. Raddi, N. P. Gentile Fusillo, T. R. Marsh, The population of hot subdwarf stars studied with *Gaia*. II. The *Gaia* DR2 catalogue of hot subluminous stars. *Astron. Astrophys.* **621**, 13 (2019).
37. B. D. Savage, T.-S. Kim, A. J. Fox, D. Massa, R. Bordoloi, E. B. Jenkins, N. Lehner, J. Bland-Hawthorn, F. J. Lockman, S. Hernandez, B. P. Wakker, Probing the outflowing multiphase gas ~1 kpc below the Galactic Center. *Astrophys. J. Suppl. Ser.* **232**, 25 (2017).
38. M. Su, T. R. Slatyer, D. P. Finkbeiner, Giant gamma-ray bubbles from *Fermi*-LAT: Active galactic nucleus activity or bipolar galactic wind? *Astrophys. J.* **724**, 1044–1082 (2010).
39. N. Melso, G. L. Bryan, M. Li, Simulating gas inflow at the disk-halo interface. *Astrophys. J.* **872**, 47 (2019).
40. D. J. Marshall, A. C. Robin, C. Reylé, M. Schultheis, S. Picaud, Modelling the Galactic interstellar extinction distribution in three dimensions. *Astron. Astrophys.* **453**, 635–651 (2006).

41. D. Krishnarao, whampy: Python package to interact with, visualize, and analyze the Wisconsin H-Alpha Mapper - Sky Survey. *J. Open Source Softw.* **4**, 1940 (2019).
42. H. S. Liszt, W. B. Burton, The gas distribution in the central region of the Galaxy. II - Carbon monoxide. *Astrophys. J.* **226**, 790–816 (1978).
43. W. B. Burton, H. S. Liszt, The gas distribution in the central region of the Galaxy. IV A survey of neutral hydrogen in the region 349 < l < 13, -10 < b < 10, |v| < 350 km/s. *Astron. Astrophys. Suppl.* **52**, 63 (1983).
44. W. B. Burton, H. S. Liszt, The gas distribution in the central region of the Galaxy. V. ^{12}CO in the direction of the Sagittarius source complex. *Astron. Astrophys. Suppl.* **95**, 9–39 (1992).
45. Gravity Collaboration, R. Abuter, A. Amorim, N. Anugu, M. Bauböck, M. Benisty, J. P. Berger, N. Blind, H. Bonnet, W. Brandner, A. Buron, C. Collin, F. Chapron, Y. Clénet, V. dCoudé u Foresto, P. T. de Zeeuw, C. Deen, F. Delplancke-Ströbele, R. Dembet, J. Dexter, G. Duvert, A. Eckart, F. Eisenhauer, G. Finger, N. M. F. Schreiber, P. Fédou, P. Garcia, R. G. Lopez, F. Gao, E. Gendron, R. Genzel, S. Gillessen, P. Gordo, M. Habibi, X. Haubois, M. Haug, F. Haußmann, T. Henning, S. Hippler, M. Horrobin, Z. Hubert, N. Hubin, A. J. Rosales, L. Jochum, L. Jocou, A. Kaufer, S. Kellner, S. Kendrew, P. Kervella, Y. Kok, M. Kulas, S. Lacour, V. Lapeyrère, B. Lazareff, J.-B. Le Bouquin, P. Léna, M. Lippa, R. Lenzen, A. Mérand, E. Müler, U. Neumann, T. Ott, L. Palanca, T. Paumard, L. Pasquini, K. Perraut, G. Perrin, O. Pfuhl, P. M. Plewa, S. Rabien, A. Ramírez, J. Ramos, C. Rau, G. Rodríguez-Coira, R.-R. Rohloff, G. Rousset, J. Sanchez-Bermudez, S. Scheithauer, M. Schöller, N. Schuler, J. Spyromilio, O. Straub, C. Straubmeier, E. Sturm, L. J. Tacconi, K. R. W. Tristram, F. Vincent, S. von Fellenberg, I. Wank, I. Waisberg, F. Widmann, E. Wieprecht, M. Wiest, E. Wiezorrek, J. Woillez, S. Yazici, D. Ziegler, G. Zins, Detection of the gravitational redshift in the orbit of the star S2 near the Galactic centre massive black hole. *Astron. Astrophys.* **615**, L15 (2018).
46. W. B. Burton, Galactic structure derived from neutral hydrogen observations using kinematic models based on the density-wave theory. *Astron. Astrophys.* **10**, 76 (1971).
47. S. R. Kulkarni, C. Heiles, Neutral hydrogen and the diffuse interstellar medium, in *Galactic and Extragalactic Radio Astronomy* (Springer, ed. 2, 1988).
48. B. T. Draine, *Physics of the Interstellar and Intergalactic Medium* (Princeton Univ. Press, 2011).
49. E. L. Fitzpatrick, D. Massa, An analysis of the shapes of interstellar extinction curves. V. The IR-through-UV curve morphology. *Astrophys. J.* **663**, 320–341 (2007).
50. G. M. Green, dustmaps: A Python interface for maps of interstellar dust. *J. Open Source Softw.* **3**, 695 (2018).
51. D. Foreman-Mackey, D. W. Hogg, D. Lang, J. Goodman, emcee: The MCMC hammer. *Publ. Astron. Soc. Pac.* **125**, 306–312 (2013).
52. L. M. Haffner, R. J. Reynolds, S. L. Tufte, WHAM observations of Hα, [S II], and [N II] toward the Orion and Perseus arms: Probing the physical conditions of the warm ionized medium. *Astrophys. J.* **523**, 223–233 (1999).
53. D. Krishnarao, L. M. Haffner, R. A. Benjamin, A. S. Hill, K. A. Barger, Warm ionized medium throughout the Sagittarius-Carina arm. *Astrophys. J.* **838**, 43 (2017).
54. Astropy Collaboration, T. P. Robitaille, E. J. Tollerud, P. Greenfield, M. Droettboom, E. Bray, T. Aldcroft, M. Davis, A. Ginsburg, A. M. Price-Whelan, W. E. Kerzendorf, A. Conley, N. Crighton, K. Barbary, D. Muna, H. Ferguson, F. Grollier, M. M. Parikh, P. H. Nair, H. M. Günther, C. Deil, J. Woillez, S. Conseil, R. Kramer, J. E. H. Turner, L. Singer, R. Fox, B. A. Weaver, V. Zabalza, Z. I. Edwards, K. A. Bostroem, D. J. Burke, A. R. Casey, S. M. Crawford, N. Dencheva, J. Ely, T. Jenness, K. Labrie, P. L. Lim, F. Pierfederici, A. Pontzen, A. Ptak, B. Refsdal, M. Servillat, O. Streicher, Astropy: A community Python package for astronomy. *Astron. Astrophys.* **558**, A33 (2013).
55. Astropy Collaboration, A. M. Price-Whelan, B. M. Sipőcz, H. M. Günther, P. L. Lim, S. M. Crawford, S. Conseil, D. L. Shupe, M. W. Craig, N. Dencheva, A. Ginsburg, J. T. V. Plas, L. D. Bradley, D. Pérez-Suárez, M. de Val-Borro; Primary Paper Contributors, T. L. Aldcroft, K. L. Cruz, T. P. Robitaille, E. J. Tollerud; Astropy Coordination Committee, C. Ardelean, T. Babej, Y. P. Bach, M. Bachetti, A. V. Bakanov, S. P. Bamford, G. Barentsen, P. Barmby, A. Baumbach, K. L. Berry, F. Biscani, M. Boquien, K. A. Bostroem, L. G. Bouma, G. B. Brammer, E. M. Bray, H. Breytenbach, H. Buddelmeijer, D. J. Burke, G. Calderone, J. L. C. Rodríguez, M. Cara, J. V. M. Cardoso, S. Cheedella, Y. Copin, L. Corrales, D. Crichton, D. D'Avella, C. Deil, É. Depagne, J. P. Dietrich, A. Donath, M. Droettboom, N. Earl, T. Erben, S. Fabbro, L. A. Ferreira, T. Finethy, R. T. Fox, L. H. Garrison, S. L. J. Gibbons, D. A. Goldstein, R. Gommers, J. P. Greco, P. Greenfield, A. M. Groener, F. Grollier, A. Hagen, P. Hirst, D. Homeier, A. J. Horton, G. Hosseinzadeh, L. Hu, J. S. Hunkeler, Ž. Ivezić, A. Jain, T. Jenness, G. Kanarek, S. Kendrew, N. S. Kern, W. E. Kerzendorf, A. Khvalko, J. King, D. Kirkby, A. M. Kulkarni, A. Kumar, A. Lee, D. Lenz, S. P. Littlefair, Z. Ma, D. M. Macleod, M. Mastropietro, C. McCully, S. Montagnac, B. M. Morris, M. Mueller, S. J. Mumford, D. Muna, N. A. Murphy, S. Nelson, G. H. Nguyen, J. P. Ninan, M. Nöthe, S. Ogaz, S. Oh, J. K. Parejko, N. Parley, S. Pascual, R. Patil, A. A. Patil, A. L. Plunkett, J. X. Prochaska, T. Rastogi, V. R. Janga, J. Sabater, P. Sakurikar, M. Seifert, L. E. Sherbert, H. Sherwood-Taylor, A. Y. Shih, J. Sick, M. T. Silbiger, S. Singanamalla, L. P. Singer, P. H. Sladen, K. A. Sooley, S. Sornarajah, O. Streicher, P. Teuben, S. W. Thomas, G. R. Tremblay, J. E. H. Turner, V. Terrón, M. H. van Kerkwijk, A. de la Vega, L. L. Watkins, B. A. Weaver, J. B. Whitmore, J. Woillez, V. Zabalza; Astropy Contributors, The astropy project: Building an open-science project and status of the v2.0 core package. *Astron. J.* **156**, 123 (2018).
56. S. van der Walt, S. C. Colbert, G. Varoquaux, The NumPy array: A structure for efficient numerical computation. *Comput. Sci. Eng.* **13**, 22–30 (2011).
57. J. D. Hunter, Matplotlib: A 2D graphics environment. *Comput. Sci. Eng.* **9**, 90–95 (2007).
58. M. Waskom, seaborn: v0.5.0. *Zenodo* (November 2014); https://zenodo.org/record/12710.
59. K. Barbary, extinction v0.3.0. *Zenodo* (2016); https://doi.org/10.5281/zenodo.804967.
60. A. Ginsburg, T. Robitaille, C. Beaumont, J. Zu Hone, spectral-cube v0.4.5. *Zenodo* (2014); https://doi.org/10.5281/zenodo.11485.

Acknowledgments: This work benefited from discussion with F. J. Lockman, N. McClure-Griffiths, B. P. Wakker, A. J. Fox, and L. D. Anderson. We thank M. Sormani for providing access to and insight on the hydrodynamical simulations used as a reference model. **Funding:** We acknowledge the support of the NSF for WHAM development, operations, and science activities. The survey observations and work presented here were funded by NSF awards AST-0607512, AST-1108911, and AST-1714472/1715623. R.A.B. would like to acknowledge support from NASA grant NNX17AJ27G. D.K. would like to acknowledge support from the J.D. Fluno Family Distinguished Graduate Fellowship. Some of this work took part under the program Milky Way Gaia of the PSI2 project funded by the IDEX Paris-Saclay, ANR-11-IDEX-0003-02. **Author contributions:** D.K. led the investigation, formal analysis, methodology, software, and visualization. R.A.B. led the conceptualization and project administration, and contributed to funding acquisition and methodology. L.M.H. led funding acquisition and resources, and contributed to project management and software. D.K. and L.M.H contributed equally to data curation; supervision was equally conducted by R.A.B. and L.M.H.; D.K., R.A.B., and L.M.H. equally contributed to validation, writing of the first draft, reviewing and editing. **Competing interests:** The authors declare that they have no competing interests. **Data and materials availability:** All data needed to evaluate the conclusions in the paper are present in the paper, the Supplementary Materials, and/or the associated GitHub repository. Additional data related to this paper may be requested from the authors.

Submitted 1 August 2019
Accepted 7 April 2020
Published 3 July 2020
10.1126/sciadv.aay9711

Citation: D. Krishnarao, R. A. Benjamin, L. M. Haffner, Discovery of diffuse optical emission lines from the inner Galaxy: Evidence for LI(N)ER-like gas. *Sci. Adv.* **6**, eaay9711 (2020).

Science Advances

Discovery of diffuse optical emission lines from the inner Galaxy: Evidence for LI(N)ER-like gas

D. Krishnarao, R. A. Benjamin and L. M. Haffner

Sci Adv **6** (27), eaay9711.
DOI: 10.1126/sciadv.aay9711